ADVANCED MATERIALS INTERFACES
www.advmatinterfaces.de

Wet-Spinning of Biocompatible Core–Shell Polyelectrolyte Complex Fibers for Tissue Engineering

*Qing Cui, Daniel Josef Bell, Sebastian Bernhard Rauer, and Matthias Wessling**

Polyelectrolyte complex fibers (PEC fibers) have great potential with regard to biomedical applications as they can be fabricated from biocompatible and water-soluble polyelectrolytes under mild process conditions. The present publication describes a novel method for the continuous fabrication of PEC fibers in a water-based wet-spinning process by interfacial complexation within a core–shell spinneret. This process combines the robustness and flexibility of nonsolvent-induced phase separation (NIPS) spinning processes conventionally used in the membrane industry with the complexation between oppositely charged polyelectrolytes. The produced fibers demonstrate a core–shell structure with a low-density core and a highly porous polyelectrolyte complex shell of ≈800 µm diameter. In the case of chitosan and polystyrene sulfonate (PSS), mechanical fiber properties could be enhanced by doping the PSS with poly(ethylene oxide) (PEO). The resulting CHI/PSS-PEO fibers present a Young modulus of 3.78 GPa and a tensile strength of 165 MPa, which is an excellent combination of elongation at break and break stress compared to literature. The suitability of the CHI/PSS-PEO fibers as a scaffold for cell culture applications is verified by a four-day cultivation of human HeLa cells on PEO-reinforced fibers with a subsequent analysis of cell viability by fluorescence-based live/dead assay.

1. Introduction

Polyelectrolyte complexes (PEC) are formed by electrostatic interactions of oppositely charged polyelectrolytes. They have attracted much attention in the pharmaceutical and biomedical field. They are promising materials for tissue engineering scaffolds, sensors and drug carriers[1–7] due to their biocompatibility and versatility in composition.[8,9] Their nontoxicity stems from their ionic nature, which renders most polyelectrolytes well water-soluble. The water solubility and ionic nature enable PEC solidification in solvent-free environments without the use of toxic additives like initiators or crosslinkers. In addition, biohybrid or completely natural materials can be fabricated, as synthetic polyelectrolytes are readily pairable with natural ones, like chitosan, alginate, or hyaluronic acid[10–12] Moreover, the vast amount of possible base polymers for polyelectrolyte complexation allows the precise adjustment of PEC properties. These include charge density, functional groups, as well as the fabrication of biodegradable materials. As a result, PECs demonstrate significant advantages compared to conventional polymers applied in the biomedical field, where materials interact with sensitive biomolecules or living cells.

These properties already led to the successful application of PECs as fibrous scaffolds, hydrogels, capsules and membrane materials.[9,10,13–22] Yim[7] developed PEC scaffolds for the precise delivery and release of various biomolecules such as bovine serum albumin (BSA), vascular endothelial growth factors (VEGF) and nerve growth factors (NGF). They were able to show that PEC fibers can be easily embedded in both a hydrophilic polysaccharide as well as a hydrophobic polycaprolactone (PCL) matrix, which improved the preservation of cargo molecules while simultaneously increasing the efficiency of sustained release. Human mesenchymal stem cells (hMSC) cultivated on NGF-loaded scaffolds showed enhanced differentiation into the neural lineage outlining the cargo release functionality of their composite scaffolds. Gomes[10] demonstrated the continuous fabrication of multicomponent PEC fibers within a Y-shaped microfluidic chip via a two-step crosslinking technique. The prepolymer solutions of chitosan and hyaluronic acid were doped with alginate and extruded into a calcium chloride bath, where alginate was ionically crosslinked by calcium ions. The alginate-fixated prepolymers were subsequently photo crosslinked by UV light to achieve stable PEC fibers. Additionally, human tendon derived cells (hTDC) were encapsulated into the hydrogel fibers to assess the applicability as tissue engineering scaffold. Their results indicate a cell viability of above 80% over 14 days of cultivation.

However, besides the major advantages and successfully developed PEC products for life-science applications, there are still many challenges with regard to the implementation of an

Q. Cui, D. J. Bell, S. B. Rauer, Prof. M. Wessling
RWTH Aachen University
Chemical Process Engineering
Forckenbeckstr. 51, 52074 Aachen, Germany
E-mail: manuscripts.cvt@avt.rwth-aachen.de
Prof. M. Wessling
DWI Leibniz-Institute for Interactive Materials
Forckenbeckstr. 50, 52074 Aachen, Germany
The ORCID identification number(s) for the author(s) of this article can be found under https://doi.org/10.1002/admi.202000849.

DOI: 10.1002/admi.202000849

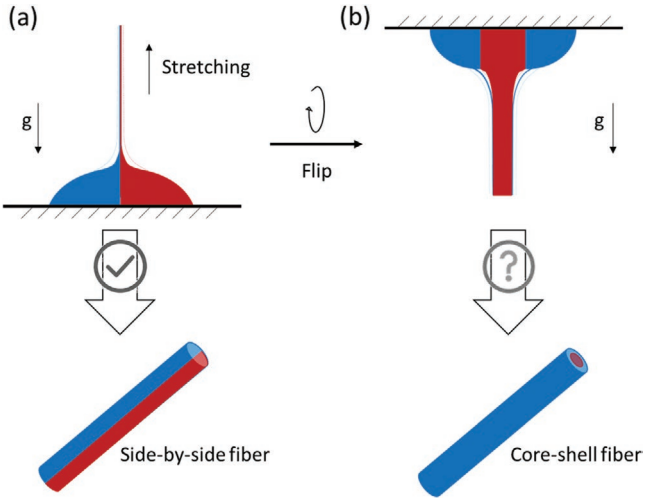

Figure 1. Scheme of PEC fiber fabrication. a) Fiber stretching from the interface of two oppositely charged polyelectrolyte droplets; b) Fiber spinning within a spinneret.

industrially feasible manufacturing method for 3D PEC scaffolds. For example, fibers synthesized from preformed PECs such as coacervates do not allow for complex fiber geometries, as the spatial distribution of polyelectrolytes cannot be controlled during the spinning process. Fabrication methods like electrospinning, hot-melt extrusion or solvent exchange,[3,23–25] which are commonly applied for processing preformed PECs, moreover expose the fiber to harsh process conditions like high temperatures or toxic solvent systems that prevent the encapsulation of sensitive biomolecules. To reduce the necessary process steps, PEC fibers can also be fabricated by in situ complexation during the spinning process, which is usually performed by microfluidic jetting[10,14] or by pulling a fiber from the interface of oppositely charged polyelectrolyte droplets[26] (**Figure 1**a). This method has been successfully applied to many polyelectrolyte pairs and even for the synthesis of multicomponent fibers composed of up to four different polyelectrolytes.[27] However, as polycation and polyanion form a complex at the fluid interface, this method is inherently restricted to the formation of side-by-side fiber geometries. Considering that droplets constitute the reservoirs for the polyelectrolyte solutions, fiber fabrication is only applicable as discontinuous processes with a low potential for scale-up. In the case of microfluidic jetting, high fluid resistances inside the microchannels as well as a demanding chip manufacturing process, pose additional obstacles to industrial implementation.

To address these challenges, we developed a novel wet-spinning process for the continuous fabrication of individual core–shell PEC fibers based on in situ interfacial polyelectrolyte complexation, which is not described in literature. Amongst the multiple driving forces involved during polyelectrolyte complexation like hydrogen bonding, hydrophobic interactions, and van der Waals interactions, the process is dominated by Coulomb interactions.[8,28] Within the developed process, fiber solidification takes place within a 3D-printed spinning nozzle (Figure 1b), and is further supported by the removal of water and excess polyelectrolytes in the washing bath, allowing for a single-step fabrication without the need for an additional coagulation bath. Considering that chitosan is well established as a cell culture substrate in literature, PEC fibers were fabricated by combining chitosan with different polyanions.[29] Additionally, crucial process parameters such as spinning rate, air gap dimension, nozzle geometry and environmental conditions, including pH, temperature and humidity, were optimized with regard to fiber stability and homogeneity. Finally, the biocompatibility of PEC fibers was assessed in a four-day cultivation of human HeLa cells on CHI/PSS-PEO fibers. A fluorescence-based live/dead assay using calcein and ethidium homodimer-1 was conducted to determine cell viability.

2. Results and Discussion

A novel wet-spinning process for the continuous fabrication of PEC fibers using a co-flow 3D printed spinning nozzle (**Figure 2**a) was developed. The nozzle closely resembles spinnerets commonly applied for the industrial fabrication of hollow fiber membranes, however, with the addition of a 10 cm long channel extension at the nozzle outlet. This modification proved to be necessary as earlier experiments using standard spinneret geometries resulted in bead formation alongside the

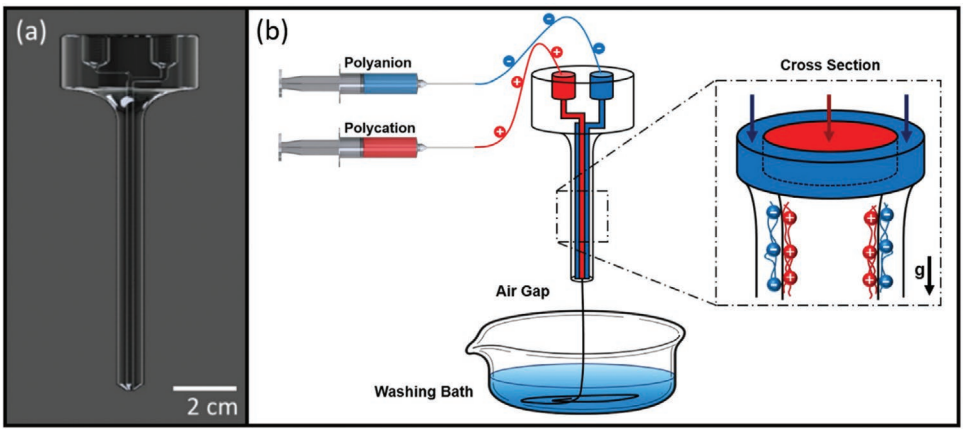

Figure 2. Scheme of spinning set-up. a) Illustration of the in-house developed spinning nozzle with inner channel diameter 0.6 mm, outer channel diameter 1.6 mm, and wall thickness 0.2 mm; b) Fiber fabrication process.

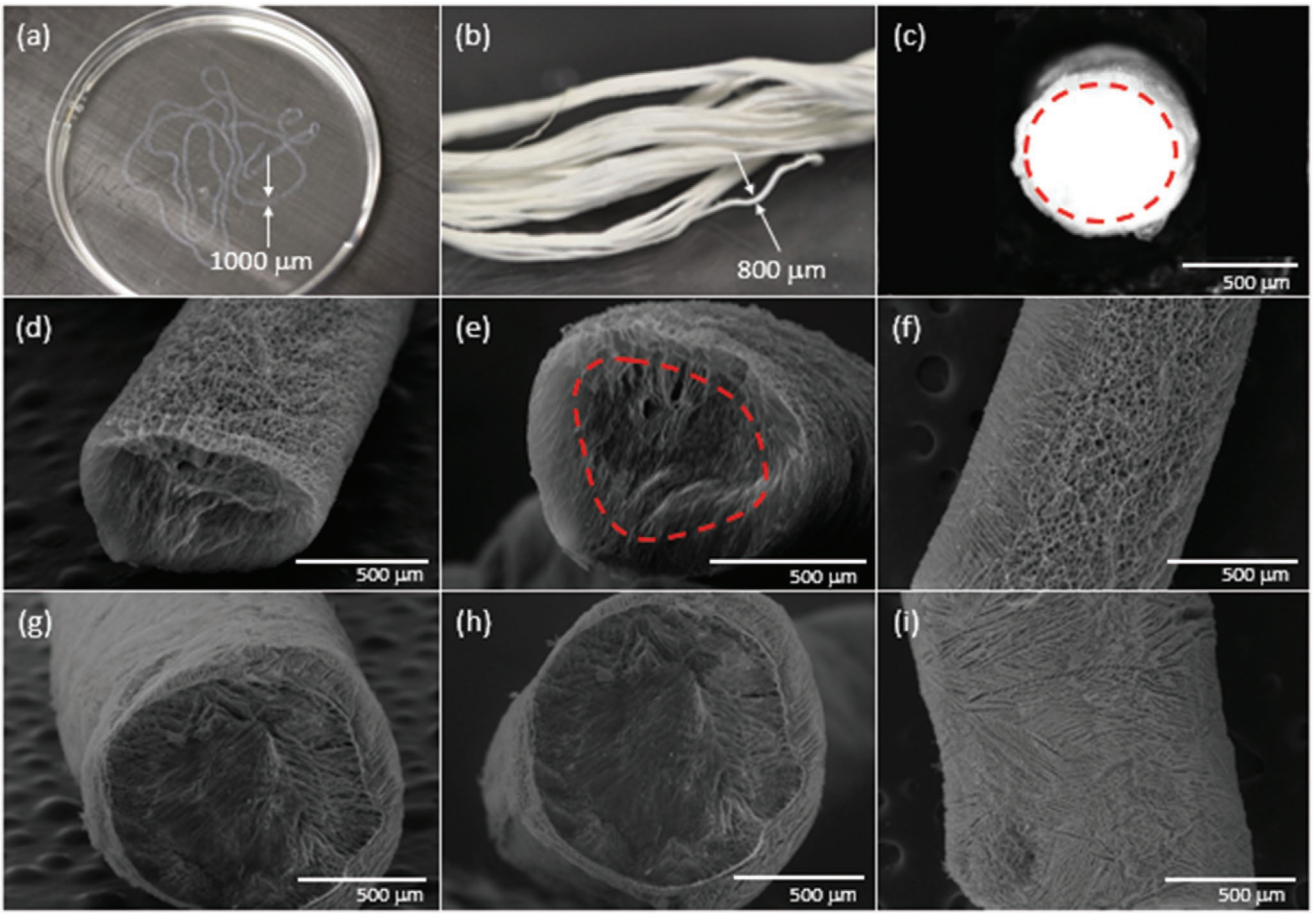

Figure 3. CHI/PSS core–shell fibers. a) Fibers in the wet state; b) Fibers after freeze drying; c) Cross-Section of freeze-dried fibers; d–f) SEM images of freeze-dried CHI/PSS fibers and g–i) SEM images of freeze-dried CHI/PSS-PEO fibers.

fiber and hence led to fiber breakage (Figure S1 in the Supporting Information as well as Videos S1 and S2 in the Supporting Information. The nozzle extension stabilizes the flow field during fiber formation and increases the contact time between the two feed solutions resulting in the complexation of the polyelectrolytes into a PEC fiber within the nozzle. Experiments with a different extension channel length of 5 and 15 cm have also led to successful fiber formation. Therefore, the intermediate length was chosen for the presented experiments. Fibers produced by our one-step wet spinning process demonstrate superior mechanical properties compared to literature allowing for the spinning of arbitrarily long fibers as well as their continuous collection on a rotating electrical drum. Furthermore, under the condition that the process takes place within the jetting regime, the fiber diameter can be adjusted between 500 and 880 µm simply by varying the flow rates of the core and shell fluid (Figure S2, Supporting Information). **Figure 3**a shows a wet CHI/PSS fiber directly after the spinning process without post-treatment, while Figure 3b depicts an identical fiber in the solid state after freeze-drying. The comparison between wet and dry diameter reveals that CHI/PSS PEC fibers swell up to 25% in aqueous solutions, where they enter a gel-like transparent state. The images of single freeze-dried CHI/PSS fibers revealed a distinct core–shell structure with a low-density core and a highly porous, uniform fiber shell (Figure 3c–f). The porosity of the fiber is a result of the freeze-drying process as schematically shown in Figure S3 in the Supporting Information.[30,31] Air drying leads to a significant shrinkage of the fibers and a loss of porosity (see Figure S4 in the Supporting Information). In addition to CHI/PSS, fibers were also successfully fabricated from a combination of CHI with poly(acrylic acid) (PAA) or poly(vinyl sulfate) (PVS) (see Figure S5 in the Supporting Information), highlighting the universality of the developed fabrication method. Both fiber types show a distinct core–shell structure with fiber dimension comparable to the CHI/PSS fibers.

FTIR and TGA analyses were performed for a qualitative and quantitative analysis of the fiber composition. **Figure 4**a shows the FTIR spectra of a CHI/PSS fiber, which exhibits the five characteristic peaks of the individual polyelectrolytes (Figure S6, Supporting Information), proving the presence of both CHI and PSS within the PEC fibers. The peaks at 3263 and 1538 $cm^{-1,}$ which indicating the N—H stretching and N—O stretching, respectively, and the C—N stretching and C—H bending signals at 1322 cm^{-1} from amino groups of CHI molecules. Another two peaks of S—O stretching at 1411 and 1037 cm^{-1} originated from sulfites of PSS molecules. The TGA spectra of CHI, PSS and a complexed fiber are depicted in Figure 4b. The degradation of pure CHI started at

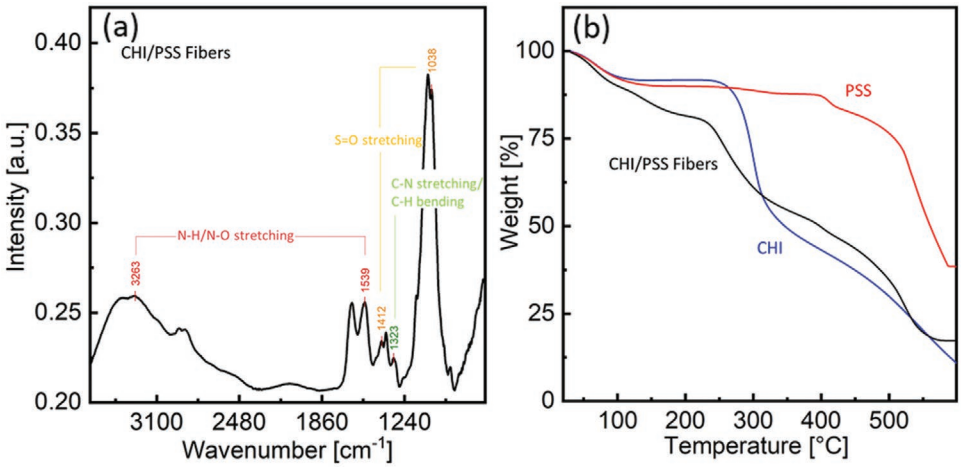

Figure 4. a) FTIR spectrum of CHI/PSS fibers; b) Weight loss curves in TGA from pure chitosan, pure PSS, and CHI/PSS fibers.

245 °C, while the first weight loss of pure PSS occurred at 400 °C. The TGA data is characteristic for the respective polymers and are in good agreement with corresponding literature.[11,32]

The TGA analysis of the CHI:PSS fiber shows three distinct regions of weight loss. In the beginning a gradual weight loss can be measured until 200 °C. This weight loss corresponds to the residual water content in the fiber, which is higher compared to the starting materials. The increased weight loss can be attributed to residual water from the spinning process, which was not removed during the drying step at ambient conditions. Water located in the 3D structure of hydrogels and PECs as loosely and tightly bound water is known to evaporate from the polymer at higher temperature ranges, which poses a possible explanation of the gradual weight loss up to 200 °C.[33,34] However, further investigation is needed in the future to support this hypothesis. A weight loss of 29% is detected when heating the sample from 230 to 390 °C. This weight loss is caused exclusively by the fiber core's CHI content, as PSS has proven to be thermally stable within this region. Pure chitosan reveals a weight loss of 51% within the same temperature interval, so that a chitosan content of ≈56% can be estimated. In the temperature range above 390 °C, an increase in weight loss can be observed. This increase can be attributed to the starting decomposition of PSS at 390 °C.

The TGA measurement reveals that the fiber is composed of nearly equal amounts of CHI and PSS with a slight excess of CHI. This ratio can be explained by the assumption that each repetitive unit of the individual polyelectrolytes has exactly one charge (i.e., CHI is maximally protonated and PSS has a pH-value independent charge). In combination with the nearly identical molecular weights of CHI and PSS per unit (CHI: 161.2 Da, PSS: 184.2 Da), PECs are likely to form with compositions of ≈1:1 (wt./wt.). In that case, the complex is electrically neutral and the excess polymer is removed by diffusion within the washing bath. The slight excess of CHI may be a result of residual CHI in the fiber core, which was not removed during the washing step.

To analyze the microscopic distribution of the polyelectrolytes within the fiber, the PSS shell solution and the core chitosan solution were labeled with fluorescent quantum dots (excitation 520 nm for PSS and 610 nm for chitosan). Confocal laser scanning microscopy was used to analyze the quantum dot distribution. **Figure 5** shows the corresponding images displaying the quantum dots in the PSS phase in green and the quantum dots in the chitosan phase in red.

The fiber surface (Figure 5a,b) shows a homogenous fluorescence signal for both quantum dots indicating a strong intermixing between the two polyelectrolytes during complexation. The spatial fiber distribution with a low-density core and a polyelectrolyte rich shell can be clearly visualized by the cross-section pictures (Figure 5c,d) in the form of a difference in fluorescence intensity between the respective fiber parts. However, there was almost no fluorescent signal of CHI-QDs in the fiber core, indicating that the polyelectrolytes migrate and aggregate at the interface leading to a low-density fiber core. The nearly hollow structure was additionally confirmed by X-ray microtomography (μCT) (Figure 5g,h) as well as Video S3 in the Supporting Information).

For the evaluation of the mechanical fiber properties, tensile tests were conducted. All measurements were performed in the dry state as wet fibers were severely damaged by the sample holder of the extensimeter. Tensile tests of the CHI/PSS fibers resulted in a Young modulus of 2.11 GPa with a tensile strength of 61.00 MPa presenting a considerable improvement compared to literature.[1,6,12,16,35–37] However, first cell culture experiments using human HeLa cells proved to be quite challenging on pure CHI/PSS fibers. When immersed in aqueous DMEM medium, the scaffolds immediately enter the swollen state, which deteriorates the handling during standard processes that use aspiration steps such as medium exchange or fluorescence staining as it renders the fibers extremely vulnerable to mechanical stress. To enhance fiber stability and simultaneously decrease scaffold swelling, the PSS spinning solution was doped with low molecular weight PEO,[38] which is known to enhance the mechanical properties of polymer systems by increasing their phase separation. The presence of PEO within the CHI/PSS-PEO fibers was verified by FTIR (**Figure 6**a). Besides the five characteristic peaks of the CHI and PSS absorbance spectra, which were already presented in Figure 4a, two new peaks became observable in the progression of CHI/PSS-PEO FTIR graph. The peaks are located at 1186 and 833 cm^{-1} and indicate C—O stretching as well as C=C bending, respectively. These deviations in the CHI/PSS-PEO

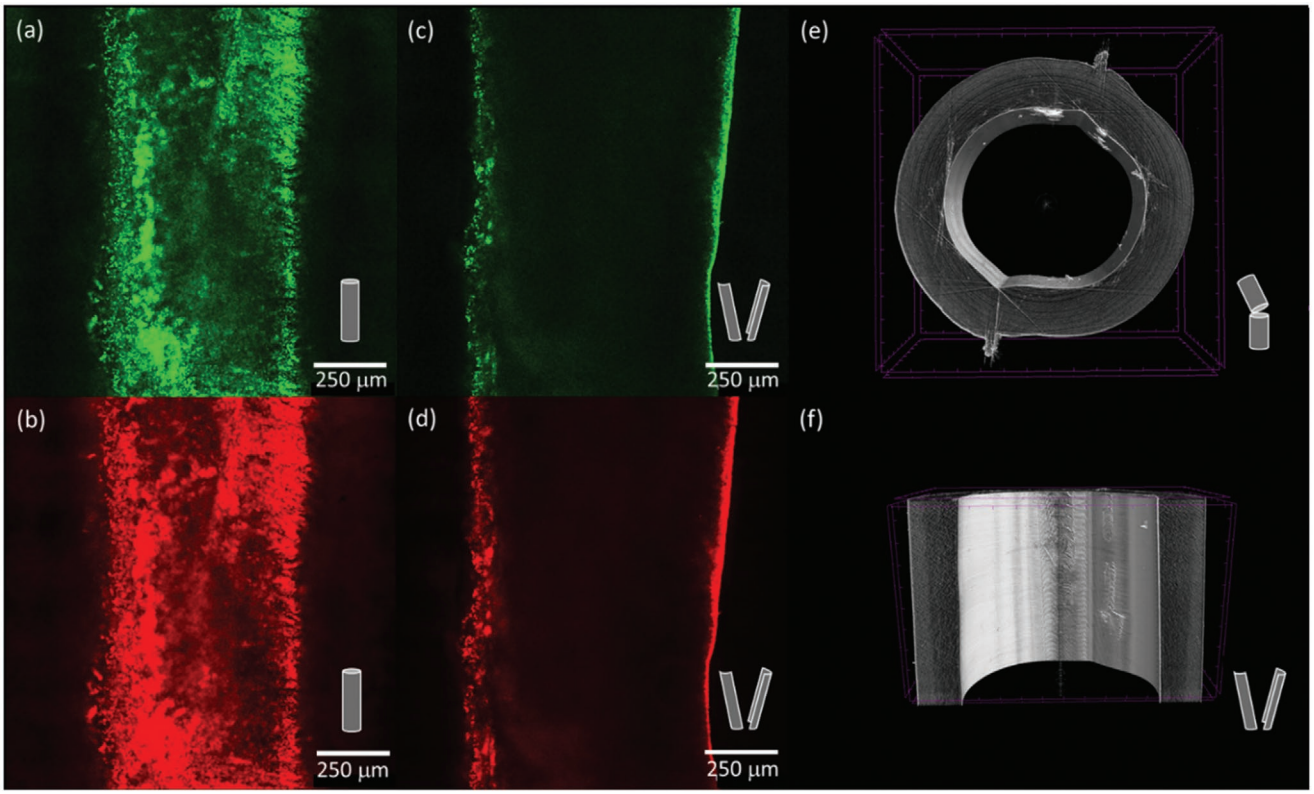

Figure 5. a,b) Surface of a CHI/PSS core–shell fiber under confocal with QDs (520 nm) in PSS and QDs (610 nm) in CHI; c,d) Cross-Section of a CHI/PSS core–shell fiber under confocal with QDs (520 nm) in PSS and QDs (610 nm) in CHI; e,f) a CHI/PSS core–shell fibers under µCT.

graph compared to the pure CHI/PSS fiber in combination with the slight increase in the O—H stretching peak located at 2917 cm^{-1} clearly indicate the successful inclusion of PEO into the PEC fiber. SEM images of the PEO doped CHI/PSS fiber revealed a core–shell structure and an increased fiber diameter compared to the nondoped CHI/PSS fibers(Figure 3g,h). Furthermore, the fiber skin is denser compared to the non-doped fiber, which is an indication for successful crosslinking (Figure 3i). Tensile tests conducted with CHI/PSS-PEO fibers could moreover verify a dopant-dependent enhancement of the elongation at break with an 80% increase in Young modulus (3.78 GPa) and a 170% increase in tensile strength (165 MPa). With regard to the application as tissue engineering scaffolds, swelling experiments were conducted in DMEM medium using the PEO-doped PEC fibers. While the diameter of pure CHI/PSS fibers reached equilibrium with a 200%-dimensional increase in only a few seconds, CHI/PSS-PEO scaffolds only swelled 110% over the duration of 18 h (**Figure 7**). This implies that PEO doping reduces both, the swelling rate as well as swelling degree.

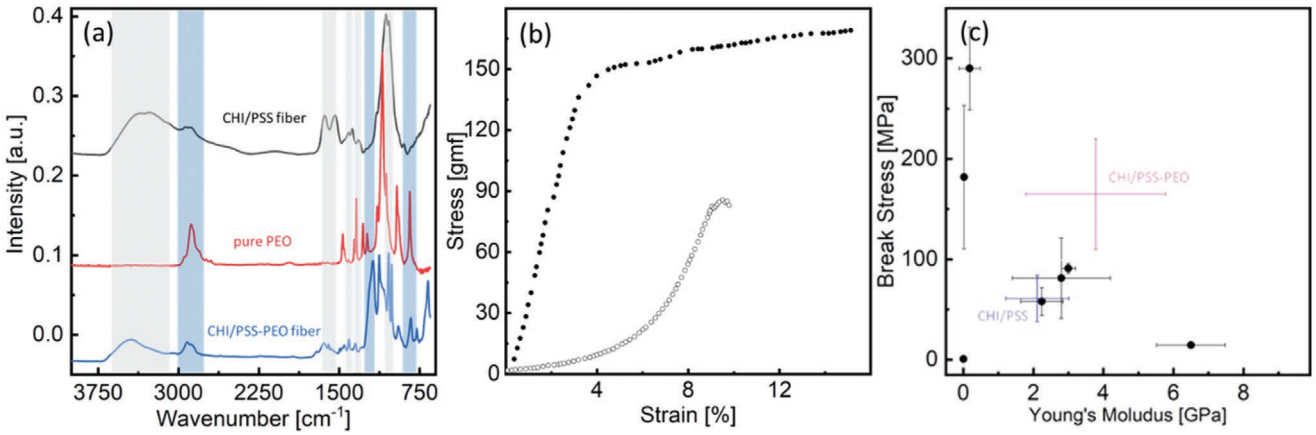

Figure 6. a) FTIR spectrum of pure PEO, CHI/PSS fibers, and CHI/PSS-PEO fibers; b) Stress–strain curves of fibers with/without PEO doping treatment; c) Mechanical properties of CHI/PSS fibers, CHI/PSS-PEO fibers compared to literature.

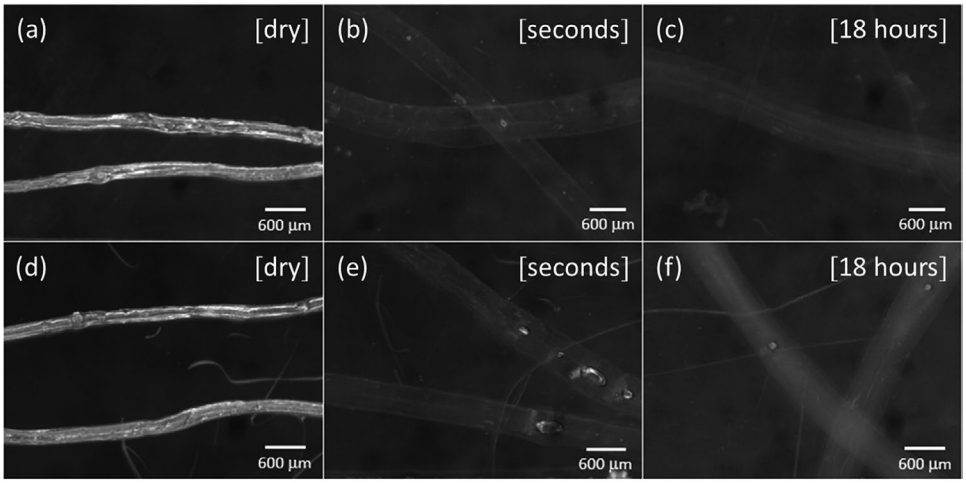

Figure 7. a–c) CHI/PSS fibers; d–f) CHI/PSS-PEO fibers; a,d) Dry fibers; b,e) Fibers immersed for seconds; c,f) Fibers immersed for 18 h.

To assess the suitability of PEO-doped scaffolds for tissue engineering applications, the cultivation of human HeLa cells was conducted. **Figure 8**a,b demonstrates live-dead confocal microscopy images of HeLa cells on CHI/PSS-PEO fibers after four days of cultivation. Dead cells are visualized in red, while living cells are depicted in green. Cell viability was determined to 81.49 ± 2.95% by manually counting the number of dead and living cells on five individual fiber samples. Considering that microscopy-based live-dead assays are only able to depict a fraction of the total cells attached to a substrate, biocompatibility was furthermore assessed globally using a cell proliferation (XTT) assay. The absorbance at 450 nm wavelength demonstrates values of 1.10 after 3 days and 0.95 after 5 days showing a stable amount of metabolically active cells. Bright-field images moreover, reveal that adhered cells are homogeneously distributed over the fiber surface and form monolayer tissue structures (Figure 8c). For evaluation of the interaction between HeLa cells and CHI/PSS-PEO substrates, cytoskeletal components, as well as proteins involved in the linkage of cells to their surrounding extracellular matrix (ECM), were studied.

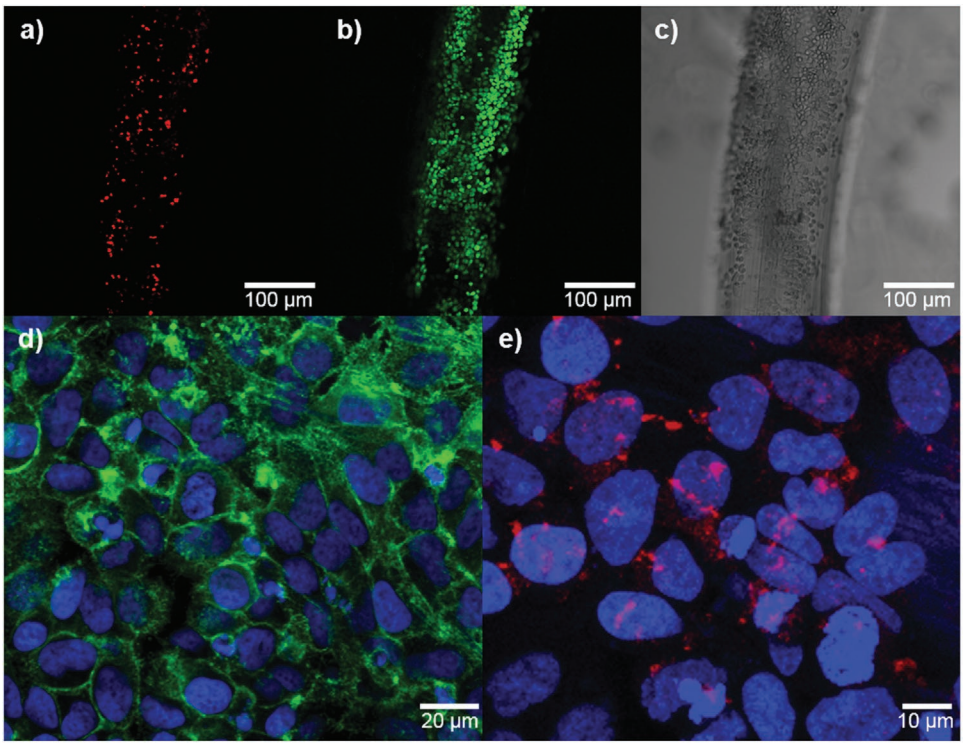

Figure 8. Human HeLa cells on a CHI/PSS-PEO fiber. a) Dead cells labeled with ethidium homodimer-1 (EthD-1). b) Living cells labeled with calcein. c) Bright field image of a cell monolayer. d) Visualization of the nuclei and actin cytoskeleton filaments by DAPI/Phalloidin staining. e) Visualization of the nuclei and focal adhesions by DAPI/Vinculin staining. Culture time: 4 d; medium: DMEM + 10% FBS + 1% PS; 37 °C humidified air 5% CO_2.

Figure 8d shows the organization of the HeLa actin cytoskeleton on PEC scaffolds. The elongation and spread of the actin filaments are a clear indicator of a high affinity of the cells to the polyelectrolyte scaffold. Additionally, the specimen was analyzed for vinculin, a membrane-cytoskeletal protein present in the integrin-actin linkage of focal adhesions (Figure 8e). The amount of vinculin (red) is proportional to the strength of cell-substrate binding.[39,40]

3. Conclusion

A novel one-step fabrication platform for the continuous production of PEC fibers (CHI/PSS, CHI/PAA, CHI/PVS) as well as PEO-doped composite fibers was developed. The process is based on a 3D-printed spinneret, which allows for stable fiber formation by guiding the complexation reaction between oppositely charged polyelectrolytes rendering an additional downstream coagulation step obsolete. The fiber composition of both, CHI/PSS, as well as CHI/PSS-PEO, was verified using FTIR and TGA. SEM, µCT and confocal microscopy imaging revealed that freeze-dried CHI/PSS fibers structurally consist of a low-density core and a dense polyelectrolyte shell that features a micrometer-sized porous morphology. The addition of PEO to the spinning solutions proved to be an effective method to improve the elongation at break, break stress and swelling behavior of PEC fibers. Tensile tests demonstrate an 80% increase in Young modulus as well as a 170% increase in tensile strength as a result of the doping procedure. The rate and degree of swelling in aqueous environments were moreover reduced significantly, enhancing the scaffold stability in the cell culture medium. Finally, biocompatibility and suitability of CHI/PSS-PEO fibers for tissue engineering applications were confirmed by a four day cultivation of human HeLa cells on PEO-doped PEC scaffolds. Life-dead analysis of the tissue structures resulted in a cell viability of 81.49 ± 2.95%. The formation of focal adhesions and the orientation of the actin filaments indicate a high affinity between cells and substrate. In the future, we envision the application of the PEC fiber spinning nozzle as a movable printing head for the fabrication of 3D PEC scaffolds.

4. Experimental Section

Materials: High molecular weight chitosan (M_w 310 000–375 000 Da, >75% de-acetylated), poly (sodium 4-styrene sulfonate) (average $M_w \approx 1\,000\,000$), poly (ethylene oxide) (average $M_w \approx 100\,000$), poly(vinylsulfonic acid, sodium salt) (30 wt% in water), cadmium telluride (CdTe) core-type quantum dots (COOH functionalized, λ_{em} 520 nm and λ_{em} 610 nm) were obtained from Sigma-Aldrich (Germany). Poly(acrylic acid) (average $M_w \approx 240\,000$, 25 wt% in water) were purchased from Acros organics. Acetic acid glacial (≥ 99.7%) and ethanol (absolute ≥ 99.8%) were purchased from VWR International. For cell culture experiments, human HeLa cells were purchased from American Type Culture Collection (ATCC). Dulbecco's Modified Eagle's Medium (DMEM) (4500 mg L^{-1} glucose, L-glutamine, sodium bicarbonate), Corning Cell Strainer (100 µm), Triton X-100, bovine serum albumin (BSA), cell proliferation kit II (XTT) and Live/Dead Cell Double Staining Kit was purchased from Sigma Aldrich. DMEM medium was supplemented with 10% Fetal Bovine Serum (FBS) from Biowest and 1% Penicillin Streptomycin (PS) from Thermo Fisher Scientific. eBioscience Anti-Vinculin (0.5 mg mL^{-1}) as well as Alexa Fluor 594 goat anti-mouse IgG (H+L) (2 mg mL^{-1}) were purchased from Thermo Fisher Scientific. Phalloidin-iFluor 488 Reagent was acquired from abcam. Paraformaldehyde (PFA) was provided by AppliChem. All washing steps were carried out using Phosphate Buffered Saline (PBS 1×) from Lonza. All listed materials were used without further purification, if not stated otherwise.

Fiber Fabrication: The spinning process was performed within a 3D printed spinning nozzle, which was prototyped by an Objet Eden 260VS 3D printer and houses two coaxial tubular channels. Fully protonated chitosan solution (1.5 wt% in 1 wt% acetic acid) and PSS solution (10 wt% in DI water) were pumped into the nozzle as core fluid and shell fluid, respectively, using two Harvard PHD Ultra Syringe Pumps (Figure 2b). Stable fiber production was achieved with a core fluid flow rate of 1.0 mL min^{-1} and a shell fluid flow rate of 0.4 mL min^{-1}. Complexed CHI/PSS fibers exiting the nozzle traveled through a 3 cm long air gap before entering a washing bath consisting of a 50:50 mixture of water and ethanol, in which the complexation process was supported by the removal of excess polyelectrolytes and water from the fiber (Figure 2b). For solidification, the fibers were subsequently freeze-dried overnight or transferred into an ethanol bath for 10 min followed by a 6 h treatment in a vacuum oven at 50 °C. For the fabrication of PEO-reinforced CHI/PSS fibers (CHI/PSS-PEO), the PSS base solution was doped with 5 wt% PEO before the spinning process. To achieve complete PEO dissolution, the solution was stirred at 360 rpm at 40 °C for 30 min.

CHI/PVS fibers were fabricated using a protonated chitosan solution (1.0 wt% in 1 wt% acetic acid) and PVS solution (30 wt% in water). The solutions were pumped into the nozzle as core fluid and shell fluid, respectively. Stable CHI/PVS fiber production was achieved with a core fluid flow rate of 1.0 mL min^{-1} and a shell fluid flow rate of 0.4 mL min^{-1}. CHI/PAA fibers were fabricated by pumping fully protonated chitosan solution (1.0 wt% in 1 wt% acetic acid) and PAA solution (25 wt% in water) into the nozzle as core fluid and shell fluid, with a flow rate 0.5 and 0.5 mL min^{-1}, respectively.

Morphology and Composition: Macroscopic analysis of the fiber morphology for wet and freeze-dried fibers was optically recorded by a Nikon D750. For fibers in the dry state, surface and cross-section morphology was moreover investigated by scanning electron microscopy (SEM) using a TM4000Plus Hitachi Tabletop Microscope. The composition of CHI/PSS fibers and single component degradation were resolved by thermo-gravimetric analysis (TGA, Netzsch TG 209). The samples were exposed to a temperature range from 30.00 °C to 800.00 °C at a step size of 10.00 °C min^{-1}. In addition, Fourier-transform infrared spectroscopy (FTIR) was conducted with both CHI/PSS fibers and CHI/PSS-PEO fibers, referenced with the spectra for pure CHI and PSS.

Structural and Mechanical Fiber Properties: The core–shell structure of CHI/PSS fibers was investigated by means of fluorescence microscopy using a TCS SP8 Leica confocal laser scanning microscope from Leica Microsystems in combination with CdTe quantum dots, which were added to the CHI and PSS base solutions prior to spinning. In addition, X-ray microtomography (µCT) was performed using a Bruker Skyscan 1272.

The mechanical properties, including Young modulus and tensile strength of CHI/PSS and CHI/PSS-PEO fibers were determined using a fiber dimensional analysis system (FDAS770) as well as an automated tensile testing system (MTT690) from Dia-Stron for a minimum of thirty samples.

Fiber Stability and Swelling in Molecularly Crowded Solutions: Dried CHI/PSS and CHI/PSS-PEO fibers were immersed in 5 mL DMEM medium supplemented with 10% FBS and 1% PS at room temperature for 18 h. The change in fiber diameter was recorded with a rapid fiber measurement system (a uEye LE USB 2.0 iDS camera, a Micro Nikkor 55 mm f/2.8 Nikon lens, and a R48 LED Ring Light from Kaiser included) built by Wessling group.

Cell Culture: Dried CHI/PSS-PEO fibers were sterilized in a 70% (v/v) ethanol-water mixture for 1 h and subsequently washed in sterile PBS (1×) for 45 min. The fibers were then transferred into Corning Cell Strainers (100 µm) and placed inside a 6-well plate for suspension culture (untreated). Human HeLa cells were seeded at a concentration

of 100.000 cells cm^{-2} in DMEM medium supplemented with 10% (v/v) FBS and 1% (v/v) PS. The samples were kept in culture for 4 days at 37 °C in an atmosphere of 5% CO_2 and 95% humidity. A medium exchange was conducted after 48 h to guarantee for sufficient nutrient supply. Prior to staining, the cultured fibers were washed three times for 1 min in sterile PBS (1×).

For the assessment of cell viability, cells were labeled applying a mixture of 0.002% (v/v) Ethidium Homodimer-1 (EthD-1) and 0.0005% (v/v) Calcein in sterile PBS (1×). The cells were incubated for 30 min at 37 °C and subsequently washed in sterile PBS (1×) for 3 min. After incubating the samples for 1 h at room temperature, cells were rinsed in PBS (1×) for 3 min.

For the analysis of the cell-scaffold interaction, additional specimens were stained for nuclei, actin and vinculin. First, the cells were fixed in 4% (v/v) paraformaldehyde solution in PBS (1×). After 15 min of incubation, the samples were permeabilized for 5 min in 0.1% (v/v) Triton X-100 in PBS (1×) and subsequently incubated in 3 wt% BSA for 1 h. Finally, the specimens were incubated in a 1:100 diluted solution of eBioscience Anti-Vinculin (0.5 mg mL^{-1}) in PBS (1×) over night. The next day, the samples were treated with a 1:200 diluted solution of Alexa Fluor 594 goat anti-mouse IgG (H+L) (2 mg mL^{-1}) and 1:1000 diluted solution of Phalloidin-iFluor 488 Reagent in PBS (1×). After two hours of incubation, 5 mg mL^{-1} DAPI staining solution was added and the specimen were incubated for additional 10 min. After each of the previously described steps, the samples were thoroughly washed with PBS (1×). Fluorescently labeled specimens were imaged with a TCS SP8 confocal laser scanning microscope from Leica Microsystems.

Biocompatibility was investigated using a Cell Proliferation Kit II (XTT) from Roche Diagnostics GmbH. The solution was prepared by mixing 5 mL of XTT labeling reagent with 0.1 mL of electron coupling reagent. To obtain reliable results, the solution was always thawed and mixed immediately before use. For XTT-analysis, the wells of a 96-wellplate for suspension culture was filled with eight 0.5 cm long fibers per well. The fibers were sterilized with 70% (v/v) ethanol-water mixture for 1 h and subsequently washed in sterile PBS (1×) for 45 min. Human HeLa cells were seeded at a concentration of 100.000 cells cm^{-2} in DMEM medium supplemented with 10% (v/v) FBS and 1% (v/v) PS. The samples were kept in culture for 5 days at 37 °C in an atmosphere of 5% CO_2 and 95% humidity. A medium exchange was conducted every 24 h to guarantee for sufficient nutrient supply. On measurement days, medium was aspirated from the respective wells and the specimens were washed twice with PBS (1×). Subsequently, 150 µL of XTT-solution was added per well and the fiber were incubated at 37 °C in an atmosphere of 5% CO_2 and 95% humidity. After 3 h of incubation, the 100 µL of supernatant was transferred to an empty 96-wellplate for suspension culture and absorbance was measured at 450 and 630 nm using a SpectraMax M3 plate reader of Molecular Devices. The respective values were corrected by subtracting the absorbance value of a blank measurement.

Supporting Information

Supporting Information is available from the Wiley Online Library or from the author.

Acknowledgements

Q.C. and D.J.B. contributed equally to this work. The work gratefully acknowledges the financial support of the China Scholarship Council. M.W. acknowledges DFG funding through the Gottfied Wilhelm Leibniz Prize 2019. The authors thank Karin Faensen for her help with μCT test.

Open access funding enabled and organized by Projekt DEAL.

Conflict of Interest

The authors declare no conflict of interest.

Keywords

cell culture, core–shell fibers, interfacial polyelectrolyte complex fibers, wet spinning

Received: May 14, 2020
Revised: October 5, 2020
Published online: October 19, 2020

[1] M. C. da Silva, H. N. da Silva, R. de C.A.L. Cruz, S. K. S. Amoah, S. M. de L. Silva, M. V. L. Fook, *Materials* **2019**, *12*, 1807.
[2] A. C. A. Wan, M. F. A. Cutiongco, B. C. U. Tai, M. F. Leong, H. F. Lu, E. K. F. Yim, *Mater. Today* **2016**, *19*, 437.
[3] N. Bhardwaj, S. C. Kundu, *Biotechnol. Adv.* **2010**, *28*, 325.
[4] J. S. Atchison, C. L. Schauer, *Sensors* **2011**, *11*, 10372.
[5] Y. Yang, T. Xia, W. Zhi, L. Wei, J. Weng, C. Zhang, X. Li, *Biomaterials* **2011**, *32*, 4243.
[6] M. Z. Albanna, T. H. Bou-Akl, H. L. Walters, H. W. T. Matthew, *J. Mech. Behav. Biomed. Mater.* **2012**, *5*, 171.
[7] M. F. A. Cutiongco, R. K. T. Choo, N. J. X. Shen, B. M. X. Chua, E. Sju, A. W. L. Choo, C. Le Visage, E. K. F. Yim, *Front. Bioeng. Biotechnol.* **2015**, *3*, 3.
[8] A. D. Kulkarni, Y. H. Vanjari, K. H. Sancheti, H. M. Patel, V. S. Belgamwar, S. J. Surana, C. V. Pardeshi, *Artif. Cells, Nanomed., Biotechnol.* **2016**, *44*, 1615.
[9] V. S. Meka, M. K. G. Sing, M. R. Pichika, S. R. Nali, V. R. M. Kolapalli, P. Kesharwani, *Drug Discovery Today* **2017**, *22*, 1697.
[10] R. Costa-Almeida, L. Gasperini, J. Borges, P. S. Babo, M. T. Rodrigues, J. F. Mano, R. L. Reis, M. E. Gomes, *ACS Biomater. Sci. Eng.* **2017**, *3*, 1322.
[11] V. B. V. Maciel, C. M. P. Yoshida, T. T. Franco, *Carbohydr. Polym.* **2015**, *132*, 537.
[12] L. Li, B. Yuan, S. Liu, S. Yu, C. Xie, F. Liu, X. Guo, L. Pei, B. Zhang, *J. Mater. Chem.* **2012**, *22*, 8585.
[13] J. Xu, R. Wu, S. Huang, M. Yang, Y. Liu, Y. Liu, R. Jiang, F. Zhu, G. Ouyang, *Anal. Chem.* **2015**, *87*, 10593.
[14] L. L. Bellan, T. Kniazeva, E. E. Kim, A. A. Epshteyn, D. D. Cropek, R. Langer, J. J. Borenstein, *Adv. Healthcare Mater.* **2012**, *1*, 164.
[15] M. Boas, A. Gradys, G. Vasilyev, M. Burman, E. Zussman, *Soft Matter* **2015**, *11*, 1739.
[16] P. Das, T. Heuser, A. Wolf, B. Zhu, D. E. Demco, S. Ifuku, A. Walther, *Biomacromolecules* **2012**, *13*, 4205.
[17] W. Tong, C. Gao, H. Möhwald, *Macromolecules* **2006**, *39*, 335.
[18] C. Gao, S. Leporatti, S. Moya, E. Donath, H. Möhwald, *Chem. - Eur. J.* **2003**, *9*, 915.
[19] C. V. Gherasim, T. Luelf, H. Roth, M. Wessling, *ACS Appl. Mater. Interfaces* **2016**, *8*, 19145.
[20] R. Shi, T. L. Sun, F. Luo, T. Nakajima, T. Kurokawa, Y. Z. Bin, M. Rubinstein, J. P. Gong, *Macromolecules* **2018**, *51*, 8887.
[21] H. Talukdar, S. Kundu, *ACS Omega* **2019**, *4*, 20212.
[22] M. Wlodek, M. Kolasinska-Sojka, M. Wasilewska, O. Bikondoa, W. H. Briscoe, P. Warszynski, *Soft Matter* **2017**, *13*, 7848.
[23] F. Ditzinger, C. Dejoie, D. S. Jung, M. Kuentz, *Pharmaceutics* **2019**, *11*.
[24] T. H. Hwang, Y. M. Lee, B. - S. Kong, J. - S. Seo, J. W. Choi, *Nano Lett.* **2012**, *12*, 802.
[25] C. Leuner, J. Dressman, *Eur. J. Pharm. Biopharm.* **2000**, *50*, 47.
[26] A. C. A. Wan, I. Liao, E. K. F. Yim, K. W. Leong, *Macromolecules* **2004**, *37*, 7019.
[27] A. C. A. Wan, M. F. Leong, J. K. C. Toh, Y. Zheng, J. Y. Ying, *Adv. Healthcare Mater.* **2012**, *1*, 101.
[28] J. Fu, J. B. Schlenoff, *J. Am. Chem. Soc.* **2016**, *138*, 980.

[29] S. Campuzano, A. E. Pelling, *Front. Sustain. Food Syst.* **2019**, *3*, 1.
[30] L. Qian, H. Zhang, *J. Chem. Technol. Biotechnol.* **2011**, *86*, 172.
[31] S. Yan, K. Zhang, Z. Liu, X. Zhang, L. Gan, B. Cao, X. Chen, L. Cui, J. Yin, *J. Mater. Chem. B* **2013**, *1*, 1541.
[32] P. Hong, S. Li, C. Ou, C. Li, L. Yang, C. Zhang, *J. Appl. Polym. Sci.* **2007**, *105*, 547.
[33] J. Ostrowska-Czubenko, M. Gierszewska-Druzyńska, *Carbohydr. Polym.* **2009**, *77*, 590.
[34] S. J. Kim, C. K. Lee, S. I. Kim, *J. Appl. Polym. Sci.* **2004**, *92*, 1467.
[35] E. N. Dresvyanina, I. P. Dobrovol'skaya, P. V. Popryadukhin, V. E. Yudin, E. M. Ivan'kova, V. Y. Elokhovskii, A. Y. Khomenko, *Fiber Chem.* **2013**, *44*, 280.
[36] L. Notin, C. Viton, L. David, P. Alcouffe, C. Rochas, A. Domard, *Acta Biomater.* **2006**, *2*, 387.
[37] M. Desorme, A. Montembault, T. Tamet, P. Maleysson, T. Bouet, L. David, *J. Appl. Polym. Sci.* **2019**, *136*, 47130.
[38] Y. Eom, B. Choi, *J. Polym. Environ.* **2019**, *27*, 256.
[39] A. A. Khalili, M. R. Ahmad, *Int. J. Mol. Sci.* **2015**, *16*, 18149.
[40] D. Lehnert, B. Wehrle-Haller, C. David, U. Weiland, C. Ballestrem, B. A. Imhof, M. Bastmeyer, *J. Cell Sci.* **2004**, *117*, 41.